Adsorption of CCl_4 on graphite

Peter W. Stephens and Martin F. Huth
Department of Physics, State University of New York at Stony Brook, Stony Brook, New York 11794
(Received 26 December 1984)

We have performed a comprehensive x-ray scattering study of CCl_4 adsorbed on exfoliated graphite. We observe the following features. At low coverages, there is an incommensurate triangular monolayer solid, with a gas-liquid-solid triple point at 195 K. Below a temperature of 215 K the graphite is partially wet by only one monolayer. The monolayer solid has a maximum melting temperature of $\sim$246 K. A two-layer solid phase, which melts at 236 K, does not have a simple triangular structure. There is a liquid prewetting film of at least ten layers thickness at 246 K, 4 K below the bulk CCl_4 triple point.

I. INTRODUCTION

There is currently great interest in quasi-two-dimensional systems formed by the physical adsorption of films having one or a few atomic or molecular layers on uniform surfaces. While many specific questions remain, it appears that the simplest, best-studied systems, namely rare gases adsorbed on graphite, are experimentally well characterized.[1] In contrast, experimental information is available on relatively few physisorbed molecules. The coupling of orientational and translational degrees of freedom leads to phases with more complicated structure than the simple triangular rare-gas solid films. In addition, the large number of possible molecular adsorbates opens the possibility of studying the systematics of various film properties. In this paper, we describe a comprehensive investigation of CCl_4 films on graphite, using x-ray diffraction to determine the structure of the film.

The present work was partly motivated by interest in the question of whether molecules with sufficiently high symmetry follow the behavior of rare gases, acting as spheres when adsorbed on graphite surfaces. It is therefore of interest to mention briefly two analogous systems, methane and CF_4. Monolayers of both isotopic forms of methane have been studied extensively; Quateman and Bretz give a brief review of recent work.[2] While expanded, compressed, and commensurate solid phases have been observed, no breakdown of triangular symmetry has been seen.[3] The current structural evidence is far from conclusive, based as it is on only one Bragg peak. Thermodynamically, Migione *et al.* found that the heat capacity of the rotational ordering transition, which occurs at 20.4 K in bulk, vanishes for films of three or four layer thickness.[4] (Of course, this could equally well be interpreted as evidence that the first few layers are always rotationally ordered due to strong substrate interactions.) The heavier system, CF_4, also exhibits three phases that can be described as strain-modulated triangular solids.[5] In this case, they are commensurate, isotropically compressed, and uniaxially compressed (striped). In addition, the monolayer phase at low temperatures has an unknown structure which is evidently more complicated than a simple triangular lattice.

Our interest is principally focused on the evolution from thin film to bulk properties. We therefore briefly review certain aspects of the current state of understanding of wetting phenomena. In a seminal paper, Pandit, Schick, and Wortis (PSW) discussed transitions from layered to bulk phases in a lattice gas model.[6] In their treatment, the key parameter was the ratio of the scale of molecule-surface attraction, u, to the scale of intermolecular attraction, v. If u/v is sufficiently large (strong substrate case), the attraction of the molecules to the substrate dominates the surface tension of the adsorbate, and the adsorbed density increases to infinity as the chemical potential approaches that of the bulk condensed phase. Each n-layer phase has a gas-liquid critical temperature, above which the density increases smoothly with chemical potential.[7] The n-layer critical temperatures approach the roughening temperature T_R for the face of the bulk crystal parallel to the substrate.[8] For somewhat smaller u/v (intermediate substrate regime), two cases are distinguished. (1) In the layering subregion, the maximum number of stable layers depends upon the temperature. Below a wetting temperature T_W, only a finite number of layers is stable for chemical potentials below bulk. Above T_W, the infinite sequence of layering transitions occurs as it does for the strong substrate case. The individual n-layer critical points approach T_R, as in the strong substrate case, and above T_R, the density increases smoothly. (2) In the prewetting subregion, the roughening temperature T_R is below the wetting temperature T_W, so that the surface is not sharp, and the number of layers in the film is not well defined. In this case, the infinite sequence of layering transitions is replaced by a single thin-film—to—thick-film transition, previously described by Cahn and by Ebner and Saam.[9]

Absent from this lattice gas picture is the influence of transitions in the bulk, which can have profound implications. For example, if the bulk triple temperature T_3 lies below the wetting temperature, it has the same effect as T_R of destroying individual layering transitions. In the prewetting subregion, T_3 then replaces T_W, so that the film thickness diverges as T_3 is approached. This is the behavior described by Mochrie *et al.* for ethylene on graphite,[10] and by Krim *et al.* for a number of gases on

Au(111).[11] In the present work we find evidence for the same phenomenon in CCl_4. Pandit and Fisher have given a more general treatment of this effect, pointing out that substrate interactions can change the relative stability of bulk phases in the neighborhood of the substrate.[12] For example, if the liquid-substrate surface tension is less than that of the solid-substrate interface, a liquid film would be stable on a surface below T_3. This would act to replace a sequence of solid layering transitions by the growth of a liquid film sufficiently near T_3.

There is currently some controversy about the wetting behavior of CF_4. From their vapor-pressure isotherms, Dolle *et al.* find evidence for incomplete wetting by two and three layers in the temperature range 77–89 K.[13] On the other hand, the LEED data of Suzanne *et al.* have been interpreted as showing a transition from incomplete wetting below 37 K, to complete wetting above that temperature.[14] If both interpretations are correct, there must be a reentrant dewetting transition between these temperatures. This may be related to structural transitions in the film, or to the phenomenon of Ref. 8.

II. PRELIMINARY DETAILS

The exfoliated graphite substrate used for this work was ~0.2 gm of Union Carbide vermicular graphite, grade GTB. This material came from the same batch as that used for the x-ray and neutron studies on ethylene.[10] The graphite was baked for 17 h at 1000 °C in a vacuum of $\sim 10^{-6}$ Torr. It was loosely packed into an all-metal cylindrical Be cell, 1.9 cm diameter by 2 cm long. The low density of the substrate may be important in controlling capillary condensation. The sample was obtained by evaporation of reagent-grade liquid CCl_4 at room temperature, following vacuum degassing.

The all-metal dosing system is similar to those used in related experiments.[10,15,16] Pressures were measured with MKS Instruments Baratron capacitance membrane manometers. Thermal transpiration is a negligible correction to any of the vapor pressures reported here. Coverages are given as gas-pressure differences in a known (primarily 50 cm^3) volume at room temperature. The sample was cooled in an Air Products Displex cryostat, with Si diode temperature sensors.

Cu$K\alpha$ x rays from a Rigaku rotating anode operating at ~7 kW were diffracted from a vertically bent pyrolytic graphite monochromator and collimated by slits before the sample. Scattered radiation was collimated by Soller slits and detected with a scintillation detector. For most of this work, the resolution was 0.009 Å^{-1} half-width at half maximum (HWHM), although it was tightened slightly to 0.007 Å^{-1} HWHM for some measurements. All data were normalized to incident flux by using a thin sheet of Kapton to scatter a small fraction of the beam before the sample into a second scintillation detector.

The surface area of the graphite sample was determined by studying the adsorption of a monolayer of Kr at 80 K. At the start of the CCl_4 studies, the Kr commensurate-incommensurate transition took place at 856±30 Torr cm^3. At the conclusion, this transition occurred at 730 Torr cm^3. One possible explanation for this 20% change in surface area is the reaction of photolytically liberated Cl with the graphite.

Scattering profiles of the Kr monolayer provide a measure of the substrate coherence length. The commensurate-phase line shape was accurately fit by a combination of Gaussian and Lorentzian line shapes suitable for finite-size limited profiles described in Ref. 15. The fitted HWHM was 0.0095±0.0005 Å^{-1}. When corrected for the 0.007 Å^{-1} HWHM spectrometer longitudinal resolution, this yields a crystallite size of 500 Å, in agreement with the much-higher-resolution measurements of Mochrie *et al.* on the same material.[10] The correlation lengths measured at the start and end of the CCl_4 runs agreed within experimental error. We find it rather surprising that the graphite substrate could have lost 20% of its surface area without noticeable degradation of the quality of its surfaces, as measured by the commensurate-phase correlation length.

We have also compared the sample used in this work to that of the ethylene experiment by Mochrie *et al.*[10] by measuring a vapor-pressure isotherm of ethylene at 103.5 K. The bottom panel of Fig. 1 shows three distinct layering transitions, in agreement with other work. In our experiments (discussed below), no more than two solid layers of CCl_4 cover the surface of graphite. The observation of a third layer of ethylene shows that this limit is not imposed by any shortcoming of the sample used here, but is intrinsic to the CCl_4-graphite system.

The empty-cell background was ~100 counts/sec, with considerable structure. During the course of the experiment, we measured the background spectrum frequently. The CCl_4 sample absorbed 5–50% of the beam, and so

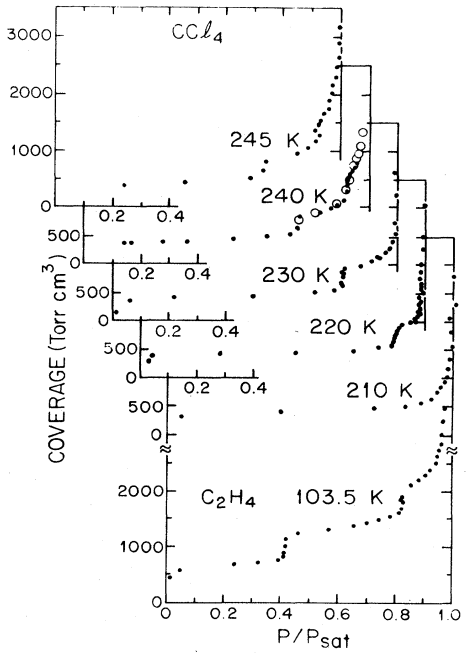

FIG. 1. Vapor-pressure isotherms of CCl_4 and ethylene on exfolilated graphite. In each case, the saturated vapor pressure P_{sat} was determined by extrapolating to infinite coverage by the Frenkel-Halsey-Hill isotherm (Ref. 17). This agreed with accepted values of saturated vapor pressure (see text). Open and solid circles at 240 K represent two separate runs.

the background had to be normalized before subtraction. On occasion, some of the sample gas condensed onto surfaces other than the graphite. A resistance heater wound around the fill line partially alleviated this problem. This was particularly acute when the sample temperature was changed with a dose of more than one monolayer, so that the gas pressure was close to that of the saturated vapor. For this reason, most of the phase diagram studies were carried out by changing dose at fixed temperature. Fortunately, it was possible to verify that the correct amount of gas was adsorbed on the surface, within a typical accuracy of 15%, by measuring the absorption of the x-ray beam by the CCl_4 in the cell. Figure 2 shows the integrated intensity of the relatively strong graphite (002) diffraction peak as a function of dose, measured during several coverage scans. For x-ray absorption by the sample gas, the intensity should be proportional to $\exp(-f/\phi)$, where f is the coverage and ϕ is the absorption constant. The lines in Fig. 2 are drawn with a common slope corresponding to $\phi = 5000 \pm 200$ Torr cm^3. Ignoring the carbon, one expects $\phi = V_s/(l_s \lambda \rho)$, where V_s and l_s are the volume and path length through the sample, λ is the mass absorption constant (103 cm^2/cm for Cl),[18] and ρ is the density of Cl in the vapor (7.6×10^{-6} gm/Torr cm^3) at room temperature. This gives $\phi = 3800$ Torr cm^3, in fair agreement with the measured value in Fig. 2.

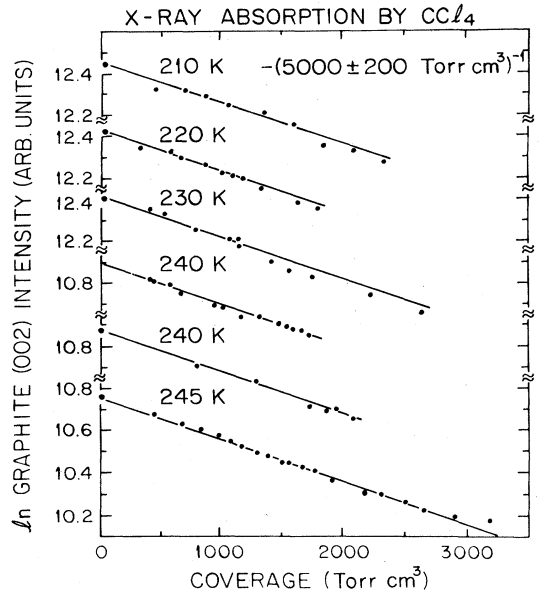

FIG. 2. Integrated intensity of the graphite (002) diffraction peak vs coverage, illustrating absorption of the x-ray beam by the CCl_4 sample. All lines are drawn with a common slope of $-(5000$ Torr cm$^3)^{-1}$.

The triple point of bulk CCl_4 is 250.3 K, where vapor, liquid, and a face-centered-cubic (fcc) solid coexist. In the fcc phase, also known as Ia, the molecules are evidently rotationally disordered. This fcc phase is metastable, and it spontaneously transforms into a structure described as rhombohedral.[19] To date, the structure of the rhombohedral phase Ib has not been solved. Below 225 K, a monoclinic phase (phase II) is stable. The structure of phase II has been solved by Cohen *et al.*[20] Rudman points out that this structure is obtained by a small distortion of the fcc structure, together with the orientational ordering of the molecules.[21] The rhombohedral Ib phase has nearly the same density as the other two, and so presumably it too is made up of a close-packed array of spheres, slightly distorted. There is a fourth solid phase which is apparently stable only at elevated pressures.[22]

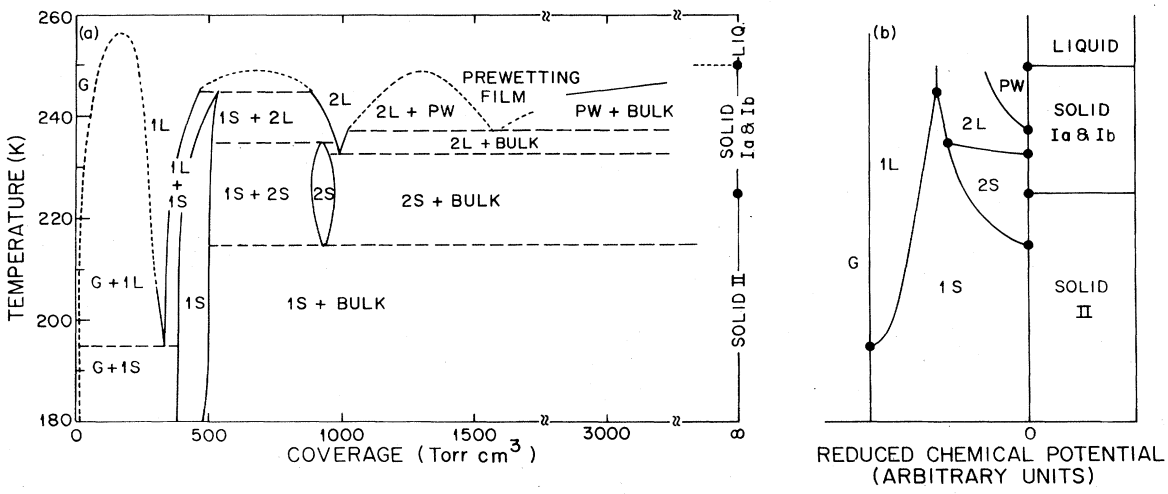

FIG. 3. (a) Proposed phase diagram for CCl_4 on graphite in the coverage-temperature plane. Long dashes indicate triple points, and short dashes indicate speculated phase boundaries. Phases are labeled as follows: G, monolayer gas phase; 1L, monolayer liquid; 1S, monolayer solid; 2L, bilayer liquid; 2S, bilayer solid; PW, prewetting film. (b) Schematic phase diagram in the chemical potential-temperature plane. The horizontal axis represents chemical potential relative to that of the bulk at each temperature.

III. EXPERIMENTAL RESULTS

In this section we present the experimental results for CCl_4 adsorbed on graphite. We show our tentative phase diagram, Fig. 3, here for reference, and defer a discussion of its specific features until we have described all of our measurements.

A. Low coverage

Diffraction line shapes observed at low coverages of CCl_4 are shown in Fig. 4. We see that for coverages of 204 and 305 Torr cm^3, a sharp diffraction peak characteristic of a two-dimensional (2D) solid occurs below 195 K, and disappears above this temperature. The scans at 101 Torr cm^3 are also consistent with this description, although the poor signal-to-noise ratio makes the interpretation somewhat less certain. When the coverage is raised to 357 Torr cm^3, the melting temperature increases to 210—220 K.

These scans provide clear evidence for a triple point in the adsorbed system in the neighborhood of 195 K. Above this temperature, a submonolayer film consists of coexisting 2D gas and liquid phases; below, gas and solid. Because the gas cannot be observed in the present scattering measurements, we observe an abrupt liquid-solid transition as the triple temperature is crossed. When the coverage is raised above that of the uncompressed liquid phase, the melting transition moves to higher temperature.

The lever law implies that the quantity of solid monolayer film should grow linearly with coverage between the densities of pure 2D vapor and solid. However, it appears that the solid-phase peaks are anomalously weak at 101 Torr cm^3, even significantly below the triple temperature. The same effect has been observed in Xe monolayers.[23] If the coexisting solid and gas phases exist on separate graphite crystallites, so that each crystallite surface is filled with one phase or the other, the solid signal should be proportional to the number of filled crystallites. On the other hand, if the coexistence occurs on individual crystallites, patches of solid could be pinned at impurities in such a way as to break up the solid, thereby producing a weaker, broader diffraction peak. Clearly, more work is required on the influence of sample heterogeneity on experiments such as this.[24]

The smooth curves in Fig. 4 are fits to a model of 2D crystallites with random orientations. As described by Heiney *et al.*, one expects a Lorentzian line shape to be an accurate description of the scattering profile from a 2D floating solid.[16] The dashed line for 357 Torr cm^3, 200 K, is a Lorentzian, powder averaged to reflect the random orientational distribution of the graphite surface.[25] This model is significantly higher than the data for wave vectors above the diffraction peak position. The discrepancy is most likely due to the form factor of the CCl_4 molecule. If one assumes that the molecules are rotating freely, the form factor is simply the Fourier transform of a spherical shell, $\sin(Qr_0)/(Qr_0)$. Taking r_0, the radius of the sphere, to be 1.75 Å (Ref. 20), we obtain the solid line. Clearly the fit is satisfactory. While this model of a triangular lattice of rotationally disordered molecules agrees with the data, we emphasize that it is by no means uniquely determined.

No other diffraction peaks are present in the neighborhood of the triple temperature. We have observed the monolayer (11) Bragg peak at temperatures of 150 K and below. Its appearance at a wave vector $\sqrt{3}$ higher than the primary peak lends further support to the interpretation that the monolayer is triangular down to the lowest temperatures studied (11 K).

The diffraction peaks shown have fitted Lorentzian half-width at half maximum (HWHM) of 0.012 ± 0.002 Å^{-1}, compared with the experimental resolution of 0.009

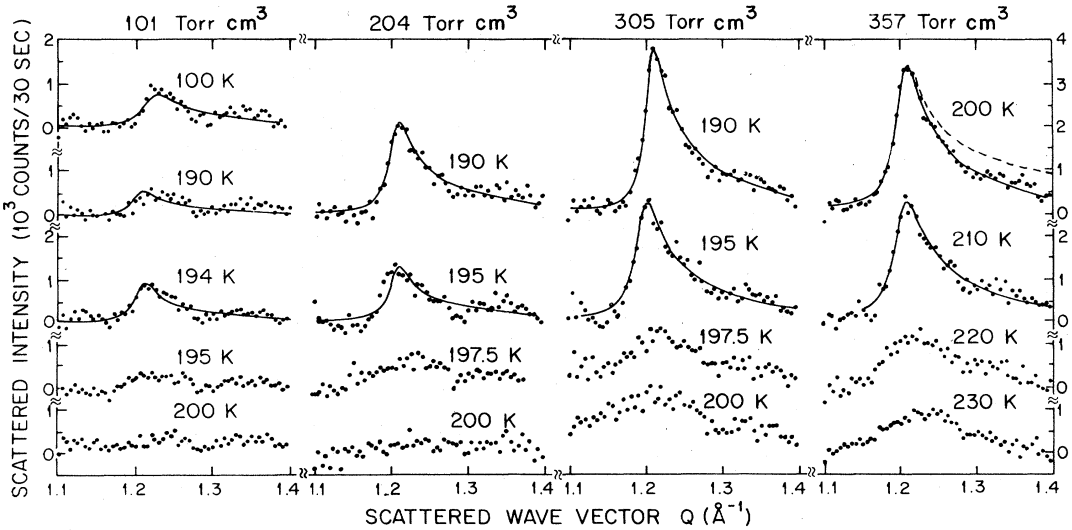

FIG. 4. Diffraction peaks at various temperatures and coverages in the submonolayer and monolayer region. The smooth curves are fits to powder-averaged Lorentzian line shapes discussed in the text. All x-ray scans reported in this paper are shown with the absorption-corrected background subtracted.

$Å^{-1}$. The deconvolution of a Lorentzian line shape with a Gaussian resolution is a complicated matter; for the purposes of a simple estimate, we assume that the widths combine in quadrature. The intrinsic peak HWHM is then 0.008 $Å^{-1}$, implying a solid crystallite size on the order of the 500 Å measured for commensurate Kr. The diffraction peak positions at the low coverages in Fig. 4 are 1.202 ± 0.002 $Å^{-1}$. The resulting intermolecular distance of 6.04 Å is slightly larger than the 5.90 Å in the bulk fcc phase stable at higher temperatures.[19]

The adsorbate is incommensurate with respect to the graphite, and quite far from any possible substrate modulation wave vector. We have not observed distortion of any of the adsorbate diffraction peaks which could be explained directly on the basis of substrate-induced strain modulation.

The measured lattice constant is a factor of 1.42 greater than that of commensurate Kr, and so one would expect the monolayer capacity to be 0.50 of that of Kr. The present observations are in agreement, with the triple point between 305 and 357 Torr cm^3, and the monolayer Kr capacity in the range 730—860 Torr cm^3.[26]

Figure 5 shows a set of scans at a coverage of 390 Torr cm^3, roughly 20% greater than the triple point. (The total dose of CCl_4 in the system was held constant; consequently the coverage changed 7% across the range of temperatures shown.) At this coverage, the solid diffraction peak has shifted to a higher wave vector, 1.22 $Å^{-1}$, indicating a compression of the monolayer solid by 2%. This implies an intermolecular separation equal to that of the fcc phase. We observe a very abrupt melting transition between 246 and 247 K, quite close to the 3D triple point of 250 K.

It is interesting to compare features of the 2D and 3D phase diagrams of CCl_4. A corresponding states argument suggests that the triple and critical temperatures of a given molecule in two and three dimensions should be in the ratio of roughly 0.5.[27] The ratio of 2D to 3D triple temperatures is nearly equal for the two classical rare gases with monolayer triple points on graphite: 0.57 for Ar (Ref. 28) and 0.61 for Xe (Ref. 23). Neon also falls into this range, at 0.55.[29] We find that the value of this ratio for CCl_4 is quite different, 0.78. Despite the fact that CCl_4 molecules appear to be freely rotating spheres in the monolayer, the principle of corresponding states does not seem to extend to this system. We speculate that this may be due to the residual entropy of orientational disorder in the solid phases.[30]

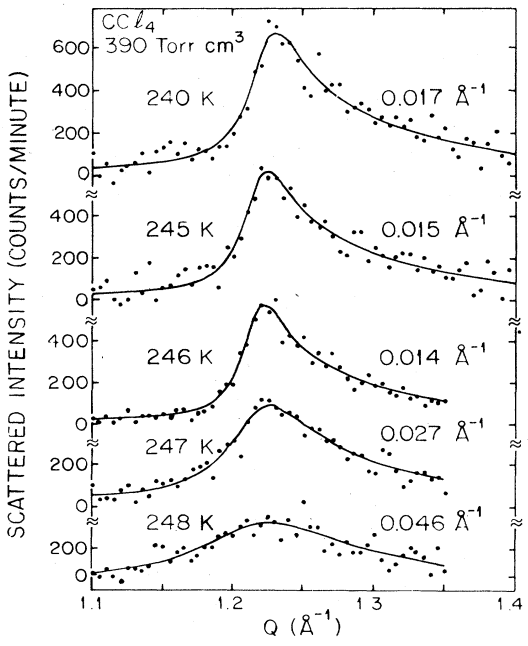

FIG. 5. Scans at approximately constant dose of 390 Torr cm^3. The fitted HWHM are listed next to each scan.

B. 210-K isotherm

Figure 6 shows the powder-diffraction patterns measured at several coverages at a constant temperature of 210 K. Both smooth curves in the bottom panel represent line-shape models discussed above. The dashed line is a fit to a powder-averaged Lorentzian, and the solid line includes the effect of the spherical molecular form factor. The 443-Torr cm^3 peak has a fitted Lorentzian HWHM of 0.014 $Å^{-1}$, compared with a spectrometer resolution of 0.009 $Å^{-1}$ HWHM.

The highest-coverage scan at this temperature is the 2323-Torr cm^3 scan shown at the top of Fig. 6. We compare this with the structure of the solid II phase stable at this temperature by showing as vertical lines the diffraction peaks measured at 195 K by Cohen *et al.*[20] There is

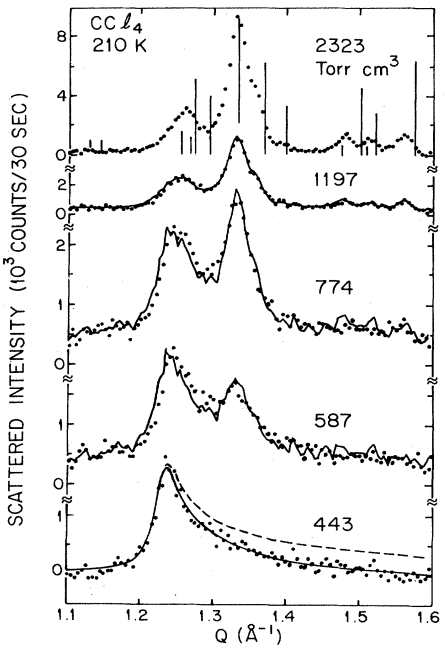

FIG. 6. Several scans at 210 K, illustrating the evolution from monolayer to bulk phases. The jagged lines through 587-, 774-, and 1197-Torr cm^3 scans are point-by-point sums of the 443- and 2323-Torr cm^3 scans, with relative weights adjusted for best fit. Vertical bars represent the positions and relative intensities of diffraction peaks measured by Cohen *et al.* in the bulk solid II phase at 195 K (Ref. 20).

crude agreement between peak positions, although the intensities differ substantially. It is possible that the small (perhaps several hundred angstroms) crystals that we observe have a different structure than the bulk phase.

The 210-K isotherm in Fig. 1 shows no steps after the condensation of the first layer, and so we expect that the cell contains a mixture of monolayer plus bulk phases at coverages above the monolayer. We test this hypothesis by fitting the intermediate-coverage scans as direct sums of the two scans at 443 and 2323 Torr cm^3.

The general procedure employed for fitting a scan as the sum of two other scans is as follows. In order to fit data $C(Q)$ as the weighted sum of $A(Q)$ and $B(Q)$ with an empty-cell background $E(Q)$, such that $C(Q)$ is approximated by $\alpha A(Q)+\beta B(Q)+\gamma E(Q)$, one minimizes the sum of the squares of the deviations,

$$\sum_i [C(Q_i)-\alpha A(Q_i)-\beta B(Q_i)-\gamma E(Q_i)]^2 .$$

This results in three simultaneous linear equations for α, β, and γ. We present the data for each scan with the absorption-corrected background, $e^{-(f/\phi)}E(Q_i)$, subtracted. Because of the monitor variability, the fitted γ fluctuates about this predicted value by $\sim 10\%$.

The jagged lines through the 587-, 774-, and 1197-Torr cm^3 scans in Fig. 6 are weighted sums of the 443- and 2323-Torr cm^3 scans. In general, they show that the description of the intermediate coverages as a combination of the two coexisting phases is correct. In the 587-Torr cm^3 scan, the monolayer peak has shifted to a wave vector of 1.237 Å^{-1}, indicating that the lattice has compressed 3% from the triple point. This wave vector implies a monolayer nearest-neighbor separation of 5.87 Å at the start of bulk phase growth. This is very close to the value of 5.90 Å characteristic of the bulk fcc phase.[19]

The values of α and β determined from the coexistence fits at 210 K are plotted in Fig. 7(a), illustrating the expected smooth tradeoff between the monolayer and bulk phases. It is possible to understand this tradeoff quantitatively as follows. Imagine that there are two phases X and Y, which would fill the sample exactly at coverages C_X and C_Y, respectively. If one has measured the scattering profile at coverages C_A, C_B, and C, with $C_X \le C_A \le C \le C_B \le C_Y$, and the three intermediate coverages are made up of lever-law coexistence of the X and Y phases, then

$$\alpha = e^{-(C-C_A)/\phi}\frac{C_B-C}{C_B-C_A}, \quad \beta = e^{(C_B-C)/\phi}\frac{C-C_A}{C_B-C_A} . \qquad (1)$$

This is the ordinary lever law between phases A and B, modified by an absorption correction. Note that this applies to cases such as the present, in which the Y phase is bulk, at essentially infinite coverage, and there is a significant amount of the low-coverage X phase present in the high-coverage experimental B scan. The smooth curves in Fig. 7(a) are calculated from Eq. (1), with absorption constant $\phi = 5000$ Torr cm^3 as discussed above.

The vapor pressure approached a value of 0.193 ± 0.01 Torr as the coverage increased.[17] Miller has calculated vapor pressures in this range of temperature by integrating other, more accurately determined, thermodynamic data.[31] He obtains 0.205 Torr at 210 K. Our measurements are therefore in agreement with the accepted saturated vapor pressure at this temperature. It is worth noting that the standard handbooks[32] quote a significantly higher value, 0.276 Torr, measured by Mundel in 1913. The difference between this value and our measurement caused great consternation until we discovered Miller's work.

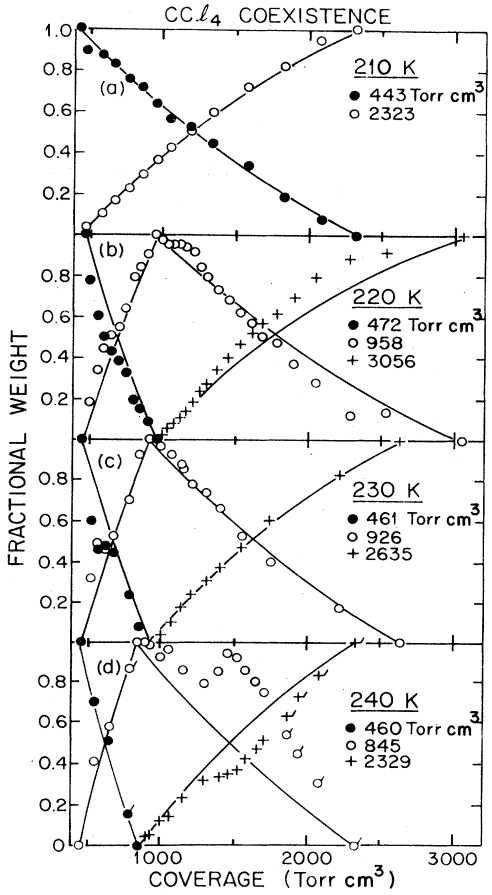

FIG. 7. Relative weights from point-by-point fits in (proposed) coexistence regions. Smooth curves are absorption-corrected lever-law models, calculated from Eq. (1). Flagged points in Fig. 7(d) are from a separate experimental run.

C. 220-K isotherm

The 220-K isotherm (Fig. 1) has a second step between roughly 550 and 950 Torr cm^3. One would therefore expect to see coexistence between one and two layers, followed by coexistence between two layers and bulk.

X-ray scans at 220 K are shown in Fig. 8. As at 210 K, the low-coverage scan is adequately described by a powder-averaged Lorentzian with the form factor for spherically disordered molecules. In contrast, we are unable to provide a simple model for the two-layer phase, here exemplified by the 958-Torr cm^3 scan. The smooth curve is the modified Warren line shape for two triangular layers first described by Kjems *et al.*[33] The Lorentzian HWHM is fixed at 0.014 Å^{-1} measured for the 472-

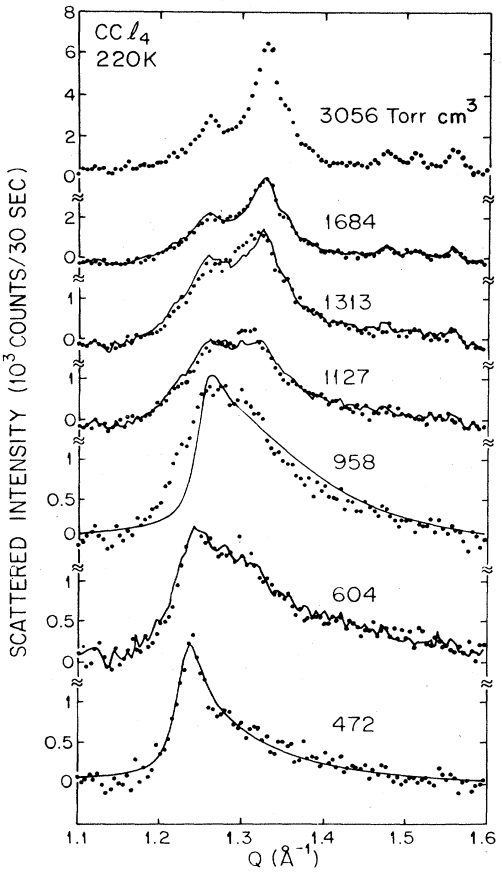

FIG. 8. Severals scans at 220 K, showing transitions from monolayer solid (472 Torr cm^3) to bilayer (958 Torr cm^3) toward bulk (3056 Torr cm^3) phases. Smooth curves through 472- and 958-Torr cm^3 scans are powder-averaged Lorentzians with spherical molecular form factor for one and two layers, respectively. Jagged curve through the 604-Torr cm^3 scan is a weighted sum of the 472- and 958-Torr cm^3 scans; curves through higher-coverage scans are weighted sums of the 958- and 3056-Torr cm^3 data.

Torr cm^3 scan. We will discuss the two-layer line shapes below. For the present purposes of point-by-point comparison of line shapes, we do not need an analytical model of the structure.

Between one and two layers, a weighted sum of 472- and 958-Torr cm^3 scans provides a satisfactory representation of the data. On the other hand, the fitted fractional weights plotted in Fig. 7(b) deviate seriously from the lever law. The 604-Torr cm^3 scan in Fig. 8 is an excellent illustration. This point is at the bottom of the steep rise in the vapor-pressure isotherm and is a 27% increase in coverage from 472 to 958 Torr cm^3, but its diffraction line shape is best fitted as 50% of each. The most likely explanation for this observation is that, as vapor pressure is increased, some capillary condensation of CCl_4 takes place. A fit to the 604-Torr cm^3 scan as the sum of the monolayer (472) and bulk (3056-Torr cm^3) scans is completely unsatisfactory, implying that the capillary-condensed phase is not the bulk phase stable at this temperature. This observation implies that there will be a contribution of the capillary-condensed material to the bilayer diffraction profile.

Point-by-point fits to coexistence between bilayer and high-coverage limit (3056 Torr cm^3) are shown in Fig. 8. In these fits, the data scans continue to show extra scattered intensity around 1.3 Å^{-1} relative to the archetypes, implying that the material responsible for this scattering between one and two layers continues to increase above bilayer coverage. An alternative explanation, that there is a three-layer phase, suffers from two disadvantages. There is no third-layer condensation visible in either the 220- or 230-K isotherms, and it leaves the excess scattering around 1.3 Å^{-1} between one and two layers unexplained. The highest-coverage scan shown at this temperature matches the highest-coverage scan at 210 K, as expected for the bulk phase II stable at these temperatures. The fitted weights, shown in Fig. 7(b), approach the high-coverage limits of zero and unity well below the highest coverage shown (3056 Torr cm^3). This could arise if the actual dose on the illuminated portion of the sample was lower than the nominal dose, measured volumetrically. We did not measure the graphite (002) peaks at high coverages in this run; thus, we do not have an independent confirmation of the dose.

The vapor pressure at this temperature approaches 0.59 Torr, again in fair agreement with Miller's value of 0.64 Torr,[31] which is slightly lower than the widely quoted 0.68 Torr.[32]

D. 230-K isotherm

The evolution from monolayer to bulk phases at 230 K is similar to that at 220 K. The data are shown in Fig. 9. The monolayer is adequately described by a Warren Lorentzian, and the bilayer is definitely not two triangular layers. Between one and two layers, the diffraction profiles fit to excessively high bilayer weight [Fig. 7(c)]. The bulk, shown in the 2635-Torr cm^3 scan, is the rhombohedral Ib form. The arrows in this scan show the allowed peak positions for a rhombohedral phase with lattice constant $a=14.5$ Å, $\alpha=90°$. At coverages intermediate between the bilayer and bulk, e.g., 1406 Torr cm^3, there is clearly less intensity in the 1.37-Å^{-1} peak and more intensity in the 1.50-Å^{-1} peak relative to the rhombohedral phase. This is what would be expected from the fcc phase, which has (111) and (200) peaks at 1.30 and 1.50 Å^{-1}, respectively. Dumas has observed that in emulsions with particle size of the order of 1 μm, the metastable fcc phase is suppressed,[34] whereas in the present case, the fcc phase is apparently enhanced for a range of coverages. It may be that the fcc phase is relatively more stable in contact with graphite, and that it is formed first in the smallest crevices, while closer to the bulk vapor pressure, crystallites of the bulk Ib phase form. With the present experimental resolution, we cannot determine whether the crystallite size as determined by the diffraction peak width changes as the Ib phase replaces the fcc.

In both the 220- and 230-K isotherms, the scattering profiles indicate the presence of another phase between the bilayer and bulk phases, even though no evidence of a

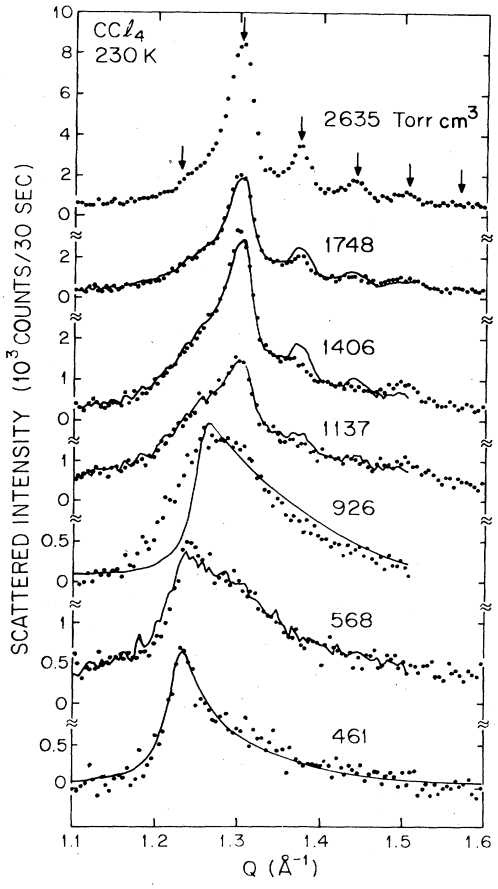

FIG. 9. Scans from isotherm at 230 K. Smooth curves through 461- and 926-Torr cm^3 scans are fits. Remaining jagged lines are point by point sums. Arrows in the highest-coverage scan are at the positions of phase Ib diffraction peaks.

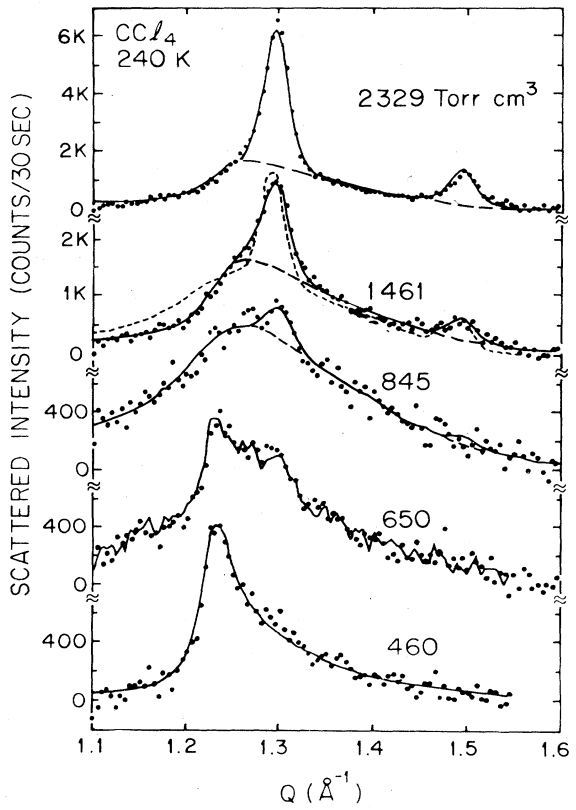

FIG. 10. X-ray scans at 240 K. The 460-Torr cm^3 scan is fit by a powder-averaged Lorentzian monolayer. The 650-Torr cm^3 scan is a weighted sum of 460- and 845-Torr cm^3 data. Remaining scans are fit as sums of powder-averaged Lorentzians plus diffraction peaks from (fcc) solid *Ia*. The short-dashed curve through 1461 Torr cm^3 is the best fit using Lorentzian parameters from the 845-Torr cm^3 fit.

third layer is seen in the vapor-pressure isotherms. It may be possible to account for this observation along the lines suggested by Pandit and Fisher,[12] who pointed out that near a bulk triple point, the relatively unstable condensed phase might preferentially wet a surface. In the present case, we may be observing the Ib or fcc phases below the Ib-II-vapor triple point because the Ib phase may have a greater affinity for the graphite surface. We never observe a Ib profile below the triple point, but this may explain the extra scattering seen around 1.3 Å^{-1} in the scans above 1000 Torr cm^3 in Fig. 8. At this and higher temperatures, the vapor pressures measured at high coverages agree with all other published data.

E. 240-, 245-, and 250-K isotherms

Several scans at 240 K are shown in Fig. 10. Again, we see a triangular solid at a monolayer coverage of 460 Torr cm^3. At a coverage of two layers, here represented by a scan at 845 Torr cm^3, the film response is considerably broader than any of the phases discussed previously. The high-coverage limit at these temperatures is well described by two sharp Bragg peaks at 1.294 Å^{-1} and 1.494 Å^{-1}, arising from the fcc solid phase, superimposed on a relatively broad peak. Both 1461 and 2329 Torr cm^3 fit the broad peak to a Lorentzian of 0.023 Å^{-1} HWHM, significantly sharper than the 0.061 Å^{-1} HWHM fitted to the 845-Torr cm^3 scan. Above 1461 Torr cm^3, the fcc Bragg peaks grow with coverage, while the broad Lorentzian remains roughly constant in intensity. It is therefore evident that the broad peak arises from the adsorbed film. However, this broad peak is significantly sharper than the bilayer 845-Torr cm^3 scan. To demonstrate that the difference in Lorentzian HWHM is significant, we show the fit to the 1461-Torr cm^3 scan as a sum of the Lorentzian fitted to 845-Torr cm^3 plus fcc Bragg peaks as a short-dashed line in Fig. 10. This model is in substantially worse agreement than the fit with Lorentzian HWHM adjusted to 0.061 Å^{-1}.

Numerical point-by-point coexistence fits reveal the same condition: scans in the range 1300—1700 Torr cm^3 fit rather poorly to the sum of the broad bilayer peak and the high-coverage limit. Perhaps more significantly, the lever-law model for the relative weights, shown in Fig. 7(d), fits the data very poorly. In view of the quantitative agreement between the lever-law model and the results of

coexistence fits shown in Fig. 7 for 210—230 K, it is clear that some change has occurred in the evolution from bilayer to bulk phases at 240 K.

We interpret this change in the structure of the adsorbed film as evidence for a prewetting transition. We shall return to this point in Sec. IV, after presenting the remaining experimental evidence.

We have not shown any of the scattering data from the 245-K isotherm because they so closely parallel that at 240 K discussed above. In order of increasing coverage, we observe the following. (1) There is a sharp triangular solid at monolayer coverage (438 Torr cm^3). (2) The bilayer phase is characterized by a large inverse correlation length of ~ 0.064 Å^{-1}. (3) As the coverage increases, the system consists of a film coexisting with fcc bulk. The film has a correlation length significantly larger than the two-layer liquid phase.

The kink around 1300 Torr cm^3 in the vapor-pressure isotherm (Fig. 1) at this temperature was caused by the cryostat becoming slightly soft. As in the 240-K data, the vapor-pressure measurements suggest the coexistence of two phases in the range 1100 to 1500 Torr cm^3, but they are not conclusive in themselves.

We also ran a vapor-pressure isotherm at 250 K on a different sample of GTB-grade exfoliated graphite with essentially the same surface area. In the vicinity of monolayer coverage, we did not observe any solid peak. Furthermore, no layering transitions were observed in the range 320—1450 Torr cm^3.

F. Bilayer structure and melting

In subsections C and D above, we have shown that there is a characteristic phase stable around two layers, which does not fit the most obvious model, that of two registered triangular layers. The scattering profiles (exemplified by the 958- and 926-Torr cm^3 scans in Figs. 8 and 9, respectively) are not made up of other coexisting phases, but instead describe a single phase of the system. At 240 K, the diffraction peak near this coverage is noticeably broader (845 Torr cm^3 in Fig. 10), suggesting that a melting transition has occurred. In order to further clarify this region of the phase diagram, we consider a series of two-layer profiles at different temperatures shown in Fig. 11.

First consider the 230-K scan in the top panel. The smooth curve is a model of a two-layer film, with the second-layer molecules in triangular sites of the first layer. In this fit, all parameters (background normalization, peak position and amplitude, and intrinsic HWHM) were adjusted, as well as the amplitude and position of a coexisting fcc solid. (The HWHM and amplitude ratio of the two fcc peaks were taken from the high-coverage fits at 240 K.) This gives an acceptable fit, with $\chi^2=1.60$, but it has an unreasonably large HWHM of 0.027 Å^{-1} for a solid phase.[35] An alternative model, with a split diffraction peak whose HWHM is fixed at the value of 0.014 Å^{-1} characteristic of monolayer solid peaks, is shown as a dashed curve. A shoulder at the position of the first peak is nearly visible in the raw data. The quality of fit is undistinguishable, with $\chi^2=1.56$ for the split sharp peaks. Fits to the 232- and 234-K scans are essentially identical

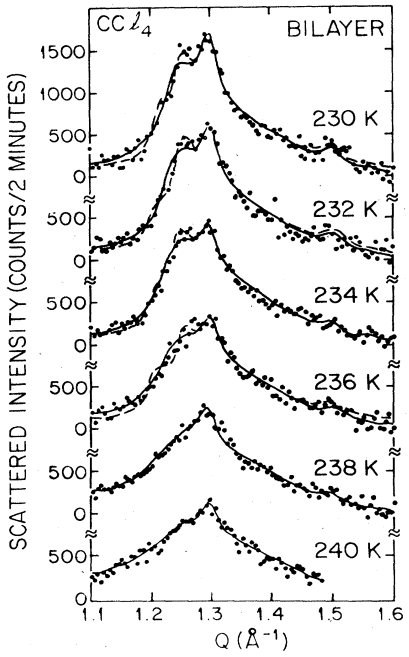

FIG. 11. Scans showing the solid structure and melting at a coverage between 892 Torr cm^3 (230 K) and 776 Torr cm^3 (240 K). The solid lines are fits to a model consisting of a 2D Lorentzian with adjustable width plus a 3D fcc solid. The dashed lines describe a model of two 2D Lorentzian peaks with HWHM fixed at 0.014 Å^{-1}, plus a 3D fcc solid.

to those at 230 K, with a single peak of HWHM $=0.027$ Å^{-1} fitting the data as well as a sharp, split peak.

The split-peak description of the diffraction profile has a natural origin as a strained triangular layer. For example, two peaks at the observed positions of 1.209 and 1.246 Å^{-1} with intensities in the observed ratio of 1:2 would be produced by a distorted triangular solid in which each molecule has two in-plane neighbors at 5.77 Å and four at 5.94 Å. Such a loss of triangular symmetry in the bilayer film could arise from the freezing of molecular orientations, as it does in the bulk solid phases of CCl_4. Of course, this description is not unique, particularly in view of the fact that the hypothesized splitting is not fully resolved. Specifically, two diffraction peaks could also arise from two mutually incommensurate triangular layers.

At 236 K, the diffraction profiles are distinctly different. The width of a single peak increases to 0.036 Å^{-1}, while the fit to two sharp peaks becomes noticeably worse. ($\chi^2=2.67$ for two sharp peaks, compared with 1.64 for one broad peak.) As the temperature is raised, the peak width increases further, to 0.074 Å^{-1} at 240 K. Evidently, the change in peak shape in the temperature range 236—240 K is the melting transition of the bilayer phase. The rapid evolution of the diffraction peak width above 236 K, considered in conjunction with its constant width for 234 K and below, leads further support to the argument that the CCl_4 film is in a solid phase below 234 K. The HWHM of 0.027 Å^{-1}, which is determined by the single-peak fits in this temperature range, is characteristic

of a disordered phase, and would therefore be expected to evolve rapidly with temperature.

This result stands in contrast to two other systems in which bilayer melting has been studied. Both He (Ref. 36) and O_2 (Ref. 37) bilayers appear to melt one layer at a time. We speculate that the difference is due to the strain which exists in the CCl_4 bilayer, but it is clear that the structure of this phase needs to be better understood before more concrete statements can be made. Complete structures, including the orientation of molecules within the unit cell, have been solved for several molecular adsorbates.[38] In the present case of an incommensurate solid at a relatively high temperature, it may be impossible to observe the higher-order Bragg peaks required for a structural analysis.

In order to observe directly the partial wetting transition between one and two layers, we sealed 849 Torr cm^3 of CCl_4 in the sample cell and lowered the temperature from 220 to 210 K. The transition from bilayer plus a small amount of bulk to monolayer film plus stronger bulk signal occurred abruptly between scans at 214 and 216 K. Upon warming, the bulk peak vanished gradually over the range 218—222 K. Mochrie *et al.* noted hysteresis of a similar reduced temperature range in their work on ethylene.[10]

G. High-coverage films

We conclude the description of experimental results with a discussion of films of many layers, close to the bulk triple point. Figure 12 shows a number of x-ray scans measured by placing a fixed dose of 3350 Torr cm^3 in the cell and varying the temperature in steps from 250 and 230 K, then back to 246 K. The absorption of the x-ray beam showed that the coverage on the graphite was 3000±300 Torr cm^3 throughout the run.

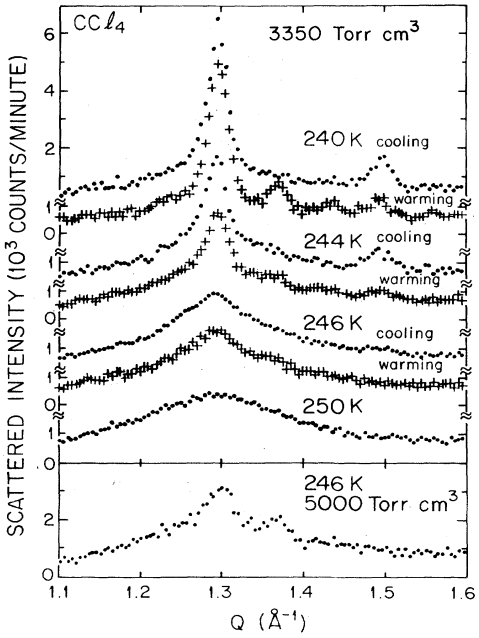

FIG. 12. X-ray scans showing the behavior of thick (approximately 10 layer) films near the bulk CCl_4 triple point.

The principal result from this run is that the CCl_4 sample is in a disordered phase at 246 K, 4 K below the bulk triple point.[39] Therefore, a film of some ten-layers thickness is fluid 4 K below the bulk triple point. Mochrie *et al.* observed a similar phenomenon in ethylene, where an eight-layer film was fluid at 103 K, 1 K below the bulk triple temperature.[10] The absence of bulk at 246 K contrasts with the isotherms performed at lower temperatures, where bulk solid appeared for all coverages above two layers. It is not the case that the bulk solid has melted, because the temperature and pressure are characteristic of solid CCl_4. Instead, it must be a consequence of the presence of the graphite substrate.

Upon further cooling to 244 K, Bragg peaks at 1.295 and 1.495 Å^{-1}, characteristic of the fcc phase, appear in coexistence with the fluid phase. The fcc solid continues to replace the fluid to 240 K. When the sample is further cooled to 230 K (not shown), it converts into the rhombohedral Ib) phase. This persists on warming to 240 K; note the Bragg peaks at 1.37, 1.435, and 1.56 Å^{-1}. When the sample is warmed to 246 K, the system is again nearly completely in a fluid phase. It is interesting to note that the transition from solid to thick fluid film occurs essentially without hysteresis, whereas the Ia to Ib conversion and the bilayer partial wetting transition are strongly hysteretic.

Bragg peaks of the rhombohedral phase start becoming evident when the coverage is increased to 5000 Torr cm^3, in the bottom panel of Fig. 12. In another run, we reached a coverage of 9800 Torr cm^3 at 245 K by cooling from above the bulk triple point. At this temperature, we observe the Ib phase with diffraction peak widths of 0.017 Å^{-1} HWHM, corresponding to a crystallite size of 200 Å after correction for resolution.

Above ~3000 Torr cm^3, a significant fraction of the CCl_4 is condensed onto some part of the sample or sample cell which was not illuminated by the x-ray beam. For example, in order to reach the coverage of 5000 Torr cm^3 at 246 K, the quantity of gas in the cell had to be raised to 8100 Torr cm^3. The amount of this missing gas depended on the thermal history of the sample. Figure 13 shows the dose adsorbed on the portion of the exfoliated graphite illuminated by x-rays as a function of time, while the temperature was changed in several steps. Generally, one observes a larger coverage at higher temperatures, but there is considerable history dependence.

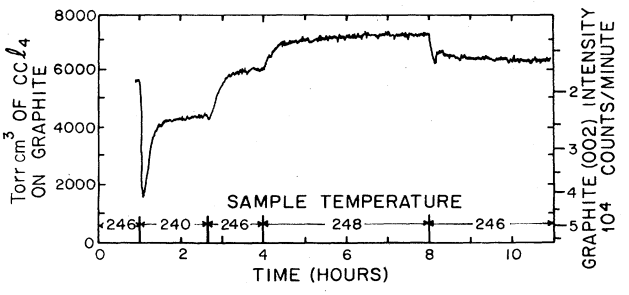

FIG. 13. Time dependence of CCl_4 dose adsorbed on graphite during several temperature steps. The sample cell contained a total of 8100 Torr cm^3.

IV. DISCUSSION

We now return to our proposed phase diagram, Fig. 3, and briefly describe the evidence for each of the features shown. The existence of a triple point between monolayer gas (G), liquid (1L), and solid (1S) phases between 300 and 357 Torr cm^3 at ~ 195 K was described in Sec. III A. We have drawn the 1L-1S transition as first order to the highest temperatures for simplicity, although it could become continuous at higher coverages. Likewise, we have no current evidence for the position of the G-1L critical point.

At 215 K, the transition from one to two solid layers meets the bulk gas-solid line. The bilayer solid (2S) does not have the structure of two layers of monolayer solid, one atop the other. The 2S phase melts at 236 K. We have drawn the phase diagram with the high-temperature extreme of 2S at a lower coverage (and therefore relative chemical potential) than the low-temperature extreme of the bilayer liquid, 2L. The opposite case, of the high-temperature limit of 2S occurring at higher coverage than the low-temperature extreme of 2L seems equally plausible; indeed one cannot rule out more complicated cases in which one phase penetrates the other or the transition is continuous.

Because of the lack of layering transitions at 250 K, we have drawn a 1L-2L critical point below this temperature. The 1S phase was observed as high as 246 K. A two-dimensional floating solid has a different symmetry from a fluid phase. Consequently, the 1S phase must have a triple point as its high-temperature limit, rather than a critical point. For this reason, we have drawn a 1L-1S-2L triple point below the 1L-2L critical point.

The existence of a thick disordered film is established by the 246-K scans in Fig. 12, where a film of ~ 10-layers thickness has no Bragg peaks, even though it is 4 K below the bulk triple point. Following the terminology of Mochrie *et al.*,[10] we have labeled this a prewetting film (PW).

Our claim that this is separated from the 2L film by a coexistence region is based on the poor fit of intermediate-coverage scans as the sum of 2L plus bulk phases, and more importantly, by the failure of the fractional weights from such fits to follow the coexistence model (Fig. 7). Of course, we cannot preclude additional layering transitions between 2L and the PW film. We do not know whether the lowest temperature of the prewetting film is above the lowest temperature of 2L, as shown, or below it, in which case there would be a 2S-2L-PW triple point.

The hysteresis noted in the different paths through the prewetting film prevents us from determining the phase boundary separating the prewetting film from its coexistence with the bulk phase. Specifically, we cannot determine whether the prewetting film thickness diverges as the bulk triple point is approached, as hypothesized by Mochrie *et al.*[10]

Our phase diagram is similar to that proposed by Mochrie *et al.* for ethylene on graphite. Specifically, the solid phases at low temperature follow the PSW (Ref. 6) intermediate substrate description, and the wetting temperature is close to the bulk triple point.

A number of unresolved issues and avenues for further research remain. The structure of the 2S phase is unknown. Perhaps high-resolution synchrotron-based measurements will resolve a diffraction peak splitting and help to elucidate this phase. Following Pandit and Fisher's description of the influence of bulk triple points on wetting phenomena, it would be interesting to study the triple point between bulk I and II phases and the 2S phase.[12] This system offers the particular advantage that all three phases have distinct diffraction profiles. One might be able to determine the G-1L, 1L-2L, and 2L-PW critical points through vapor-pressure isotherms. Finally, we believe that the most important open question is the nature of the prewetting film as it approaches the bulk triple point. While the description advanced by Mochrie *et al.* for ethylene on graphite, that the bulk triple temperature equals the wetting temperature, provides a simple description of the ethylene and CCl_4 phase diagrams, it is not directly proven for either system.

ACKNOWLEDGMENTS

We are grateful to R. J. Birgeneau and R. B. Griffiths for useful discussions, to R. Rudman for pointing out several references and furnishing unpublished data, and to P. Heiney for a careful reading of this manuscript. L.-D. Chang and Y. Chou helped set up equipment, and B. Ovryn participated in some of the preliminary measurements on CCl_4. We also thank R. Fleming for providing x-ray-spectrometer control software. The sample of GTB-grade exfoliated graphite was kindly provided by M. Dowell of Union Carbide. This work was supported by the Research Corporation and by the National Science Foundation Low Temperature Physics program under Grant No. DMR 8208570.

[1]See, for example, *Ordering in Two Dimensions,* edited by S. K. Sinha (North-Holland, New York, 1980); *Phase Transitions in Surface Films,* edited by J. G. Dash and J. Ruvalds (Plenum, New York, 1980).

[2]J. H. Quateman and M. Bretz, Phys. Rev. B **29**, 1159 (1984).

[3]P. Vora, S. K. Sinha, and R. K. Crawford, Phys. Rev. Lett. **43**, 704 (1979).

[4]A. D. Migone, M. W. H. Chan and J. R. Boyer, Physica **108B**, 787 (1981).

[5]K. Kjaer, M. Nielsen, J. Bohr, H. J. Lauter, and J. P. McTague, Phys. Rev. B **26**, 5168 (1982).

[6]R. Pandit, M. Schick, and M. Wortis, Phys. Rev. B **26**, 5112 (1982).

[7]This was first discussed theoretically by M. J. de Oliveira and R. B. Griffiths, Surf. Sci. **71**, 687 (1978).

[8]For sufficiently large u/v, a number of systems revert to partial wetting. J. L. Seguin, J. Suzanne, M. Bienfait, J. G. Dash, and J. A. Venables, Phys. Rev. Lett. **51**, 122 (1983); M. Bienfait, J. L. Seguin, J. Suzanne, E. Lerner, J. Krim, and J. G. Dash, Phys. Rev. B **29**, 983 (1984).

[9]J. W. Cahn, J. Chem. Phys. **66**, 3667 (1977); C. Ebner and W. F. Saam, Phys. Rev. Lett. **38**, 1486 (1977).

[10]S. G. J. Mochrie, M. Sutton, R. J. Birgeneau, D. E. Moncton, and P. M. Horn, Phys. Rev. B **30**, 263 (1984).

[11]J. Krim, J. G. Dash, and J. Suzanne, Phys. Rev. Lett. **52**, 640 (1984).

[12]R. Pandit and M. E. Fisher, Phys. Rev. Lett. **51**, 1772 (1983).

[13]P. Dolle, M. Matecki, and A. Thomy, Surf. Sci. **91**, 271 (1980).

[14]J. Suzanne, J. L. Seguin, M. Bienfait, and E. Lerner, Phys. Rev. Lett. **52**, 637 (1984).

[15]P. W. Stephens, P. A. Heiney, R. J. Birgeneau, P. M. Horn, D. E. Moncton, and G. S. Brown, Phys. Rev. B **29**, 3512 (1984).

[16]P. A. Heiney, P. W. Stephens, R. J. Birgeneau, P. M. Horn, and D. E. Moncton, Phys. Rev. B **28**, 6416 (1983).

[17]We extrapolated to saturated vapor pressure using the Frenkel-Halsey-Hill isotherm, $P(n)=P_{\rm sat}\exp(-An^{-3})$. This describes a film of structureless material bound to a substrate by the van der Waals attraction. It has no direct justification in the present case, but it provides a well-defined functional form for extrapolation. See J. G. Dash, *Films on Solid Surfaces* (Academic, New York, 1975).

[18]*X-ray Diffraction by Polycrystalline Materials,* edited by H. S. Peiser, H. P. Rooksby, and A. J. C. Wilson (IOP, London, 1955).

[19]R. Rudman and B. Post, Science **154**, 1011 (1966); Mol. Cryst. **5**, 95 (1968).

[20]S. Cohen, R. Powers, and R. Rudman, Acta Crystallogr. Sect. B **35**, 1670 (1979).

[21]R. Rudman, Solid State Commun. **29**, 785 (1979).

[22]V. E. Bean and S. D. Wood, J. Chem. Phys. **72**, 5838 (1980).

[23]E. M. Hammonds, P. Heiney, P. W. Stephens, R. J. Birgeneau, and P. Horn, J. Phys. C **13**, L301 (1980); R. J. Birgeneau, E. M. Hammonds, P. Heiney, P. W. Stephens, and P. M. Horn, in *Ordering in Two Dimensions,* edited by S. K. Sinha (North-Holland, New York, 1980).

[24]The effect of heterogeneity on monolayer phase transitions has been considered by J. G. Dash and R. D. Puff, Phys. Rev. B **24**, 295 (1981), and by R. E. Ecke, J. G. Dash, and R. D. Puff, *ibid.* **28**, 1288 (1982). Their model assumed a length scale of energy inhomogeneities greater than the correlation length of the solid. In the present case, it appears that we are observing the opposite limit. A description in terms of quenched random fields may be more appropriate; see, e.g., R. A. Cowley, R. J. Birgeneau, G. Shirane, and H. Yoshizawa, in *Multicritical Phenomena,* edited by R. Pynn and A. Skjeltorp (Plenum, New York, 1983) for a review.

[25]Reference 15 gives an extensive discussion of line-shape models for 2D systems adsorbed on powders.

[26]Direct comparison of the CCl_4 triple point and the Kr commensurate-incommensurate transition coverage is complicated by the presence of thermally activated vacancies, interstitial atoms, and promotion to the second layer.

[27]A review of the pertinent critical-point data is given by J. G. Dash, *Films on Solid Surfaces* (Academic, New York, 1975).

[28]J. P. McTague, J. Als-Nielsen, J. Bohr, and M. Nielsen, Phys. Rev. B **25**, 7765 (1982).

[29]G. B. Huff and J. G. Dash, J. Low Temp. Phys. **24**, 155 (1976); H. Wiechert, G. Tilby, and H. J. Lauter, Physica **108B**, 785 (1981).

[30]The ratio of 2D to 3D triple temperatures in CF_4 is 0.84, close to the value of 0.78 found here for CCl_4. In this case, a comparison is risky, because the solid phase of CF_4 is commensurate with the graphite substrate, which has an important effect on the monolayer solid.

[31]G. A. Miller, J. Chem. Engin, Data **7**, 353 (1962).

[32]*Handbook of Chemistry and Physics,* 64th ed., edited by R. C. Weast (Chemical Rubber Co., Boca Raton, Fla., 1983); C. F. Mundel, Z. Phys. Chem. **85**, 435 (1913).

[33]J. K. Kjems, L. Passell, H. Taub, J. G. Dash, and A. D. Novaco, Phys. Rev. B **13**, 1446 (1976).

[34]J. P. Dumas, J. Phys. C **12**, 2225 (1979).

[35]We define χ^2 as $\sum_i[(y_i-Y_i)^2/y_i]/(N-m-1)$, where the sum runs over the N data points of the experimental scan y_i, and Y_i is the calculated model having m adjustable parameters. If the data were described perfectly by the model, with deviations due only to counting statistics, χ^2 would be approximately one.

[36]M. Bretz, Phys. Rev. Lett. **31**, 1447 (1973); K. Carneiro, L. Passell, W. Thomlinson, and H. Taub, Phys. Rev. B **24**, 1170 (1981).

[37]S. G. J. Mochrie, M. Sutton, J. Akimitsu, R. J. Birgeneau, P. M. Horn, P. Dimon, and D. E. Moncton, Surf. Sci. **138**, 599 (1984).

[38]See, e.g., J. P. Coulomb, J. P. Biberian, J. Suzanne, A. Thomy, G. J. Trott, H. Taub, H. R. Danner, and F. Y. Hansen, Phys. Rev. Lett. **43**, 1878 (1979); R. Wang, H. Taub, H. Schechter, R. Brener, J. Suzanne, and F. Y. Hansen, Phys. Rev. B **27**, 5864 (1983).

[39]We explicitly verified the temperature calibration at the end of this temperature scan by measuring a sample pressure of 5.63 Torr, which is the saturated vapor pressure at 244.5±0.5 K (Refs. 31 and 32).